KIF3A/B: A Heterodimeric Kinesin Superfamily Protein That Works as a Microtubule Plus End–directed Motor for Membrane Organelle Transport

Hiroto Yamazaki, Takao Nakata, Yasushi Okada, and Nobutaka Hirokawa

Department of Anatomy and Cell Biology, Faculty of Medicine, University of Tokyo, Tokyo 113, Japan

Abstract. We cloned a new member of the murine brain kinesin superfamily, KIF3B, and found that its amino acid sequence is highly homologous but not identical to KIF3A, which we previously cloned and named KIF3 (47% identical). KIF3B is localized in various organ tissues and developing neurons of mice and accumulates with anterogradely moving membranous organelles after ligation of nerve axons. Immunoprecipitation assay of the brain revealed that KIF3B forms a complex with KIF3A and three other high molecular weight ($\sim$100 kD)–associated polypeptides, called the kinesin superfamily–associated protein 3 (KAP3). In vitro reconstruction using baculovirus expression systems showed that KIF3A and KIF3B directly bind with each other in the absence of KAP3. The recombinant KIF3A/B complex ($\sim$50-nm rod with two globular heads and a single globular tail) demonstrated plus end–directed microtubule sliding activity in vitro. In ad-
dition, we showed that KIF3B itself has motor activity in vitro, by making a complex of wild-type KIF3B and a chimeric motor protein (KIF3B head and KIF3A rod tail). Subcellular fractionation of mouse brain homogenates showed a considerable amount of the native KIF3 complex to be associated with membrane fractions other than synaptic vesicles. Immunoprecipitation by anti-KIF3B antibody–conjugated beads and its electron microscopic study also revealed that KIF3 is associated with membranous organelles. Moreover, we found that the composition of KAP3 is different in the brain and testis. Our findings suggest that KIF3B forms a heterodimer with KIF3A and functions as a new microtubule-based anterograde translocator for membranous organelles, and that KAP3 may determine functional diversity of the KIF3 complex in various kinds of cells in vivo.

A mature neuronal cell has a polarized morphology comprised of dendrites, a long axon, and synapses. Most of the proteins in the axon and synapses must be transported from the cell body along the axon because it lacks protein synthesis machinery. Various kinds of proteins are bidirectionally transported by fast and slow axonal flow, and fast transport is primarily responsible for moving the membranous organelles. Kinesin is a microtubule-activated ATPase (Brady, 1985; Vale et al., 1985*a*; Scholey et al., 1985) that moves to the plus end of microtubules (Vale et al., 1985*b*; Saxton et al., 1988). Since this protein was shown to be associated with membranous organelles anterogradely moving in the axon (Hirokawa et al., 1991), it is therefore considered a leading candidate to be the anterograde motor. EM studies on axons in vivo have shown that cross-bridge structures exist between the membranous organelles and microtubules, which are consistent in size and shape with the single-molecule structure

of kinesin (Hirokawa et al., 1989). On the other hand, we also identified several distinct cross-bridge structures that are also candidates to be membranous organelle motors (Hirokawa, 1982; Hirokawa and Yorifuji, 1986). Obviously, then, a possibility exists that a number of different motor proteins are engaged in fast axonal transports.

Many kinds of kinesin-like motor proteins have recently been found and cloned (for review see Endow, 1991; Goldstein, 1991; Hirokawa, 1993), and all members share a homologous domain having $\sim$350 amino acids and containing a site for putative ATP binding and one for microtubule binding. This superfamily of kinesin-like microtubule-based motor proteins is thought to have diverse motility functions such as mitosis and meiosis. To identify new molecular motors for organelle transport, we have already cloned five members of the kinesin superfamily (KIF1-5) from murine brain (Aizawa et al., 1992). In the previous study, we showed that KIF3A (formerly designated KIF3) is predominantly expressed in the brain and is a new motor protein for anterograde fast axonal transport (Kondo et al., 1994).

In this study we have cloned a new member of the kine-

sin superfamily other than those reported previously (Aizawa et al., 1992), and subsequent sequencing revealed that it is homologous but distinct from KIF3A. Chlonological and spatial expression pattern of this new motor protein, KIF3B, was closely related with KIF3A, which leads to speculation that KIF3A and KIF3B are associated with each other. Then we found that KIF3A, KIF3B, and their associated proteins make a complex in vivo by immunoprecipitation. Detailed investigations of the KIF3 complex were carried out using molecular biological, immunocytochemical, and biochemical approaches, that is, EM of its molecular structure and a microtubule sliding assay were performed using a baculovirus-expressed KIF3A/B complex, while its accumulation was examined by ligating peripheral nerves. Taken together, our findings suggest that the KIF3 complex is another microtubule-based motor protein that participates in anterograde fast axonal transport for membranous organelles in neurons. In addition, we demonstrate that this complex is a heterodimeric motor protein having associated proteins in mammalian cells. We named these associated proteins kinesin superfamily–associated protein 3 (KAP3).[1]

Materials and Methods

Cloning of KIF3B

Construction of the λgt10 library from poly(A) RNA of 0-d-old murine brains and PCR to amplify the conserved segment of cDNAs of kinesin superfamily members was performed, as previously described. (Aizawa et al., 1992; Nakata et al., 1993). A PCR fragment of KIF3B was used as a probe to screen the cDNA library according to the standard method, and a full-length of KIF3B cDNA was sequenced by the dideoxynucleotide chain termination method.

Northern Blot Analysis

Total RNA was prepared, as described previously (Aizawa et al., 1992). mRNA was purified from total RNA using Oligotex-dT30<super> (Takara, Kyoto, Japan). The amount of mRNA was determined by measuring the absorbance at 260 nm and adjusted by preliminary Northern blot analysis using the radioactivity from a β-actin probe. The mRNA sample (1–2 μg) was electrophoresed and transferred to a nylon filter, and hybridization was performed, as described previously (Aizawa et al., 1992). For hybridization probes to detect mRNA of KIF3A and KIF3B, we respectively used the HincII/PstI cDNA fragment of KIF3A (1,024 bp) and the EcoRI/BamHI cDNA fragment of KIF3B (1,101 bp).

Construction of Transfer Vector and Purification of Recombinant KIF3B

A transfer vector was constructed using the pBacPAK8 transfer vector (BacPAK Baculovirus expression system; Clonetech Inc., Palo Alto, CA). To generate pBacPAK8/KIF3B containing the polyhistidine tag, we used the PCR method with Taq polymerase to introduce in-frame six histidine codons and a stop codon in the COOH terminus. pBacPAK8/KIF3B was finally used for transfection to obtain recombinant baculovirus containing KIF3B cDNA.

The methods of transfection and selection of recombinant KIF3B virus were as described previously (Kondo et al., 1994). Infected cells were resuspended in binding buffer (10 mM imidazole, 0.5 M NaCl, 20 mM Tris HCl, pH 7.9) supplemented with protease inhibitor mixtures. The cells were then lysed with a glass–teflon homogenizer and clarified by ultracentrifugation (Beckman TL100) at 100,000 g for 30 min. The resultant supernatant was purified using a chelating Sepharose FF column (nickel col-

umn) (Pharmacia Inc., Piscataway, NJ) according to the manufacturer's instructions. KIF3B was subsequently eluted with the elution buffer (1 M imidazole, 0.5 M NaCl, 20 mM Tris-HCl, pH 7.9). Typically, 0.4 mg of protein with >95% purity was obtained from 10^8 cells.

Antibody Preparation and Affinity Purification

To produce an antibody against KIF3B, the recombinant full-length KIF3B protein was used. Purified KIF3B was injected into rabbits four times and the rabbits were bled. The serum was then affinity purified using a KIF3B-bound activated Thiol-Sepharose 4B affinity column (Pharmacia Inc.). Western blotting of the final antibodies was carried out to confirm no cross-reaction with KIF3A. For the motility inhibition assay, purified antibodies were dialyzed against a PEM buffer (0.1 M Pipes, pH 6.8, 1 mM EGTA, 1 mM MgCl₂).

Western Blot Analysis

Various mouse tissues (0.1 mg each) were homogenized into 400 μl of sample buffer and boiled for 3 min. Crude homogenates (5 μl each) were fractionated on SDS-PAGE and transferred to an immobilon membrane (Millipore Corp., Bedford, MA). The filters were used for the Western blotting as described previously (Kondo et al., 1994). The bound antibody was detected with ¹²⁵I-labeled protein A.

Immunofluorescence Microscopy

The cerebrum, cerebellum, and hippocampus of 8-wk-old mice were processed for immunofluorescence microscopy using affinity-purified anti-KIF3B antibody as described previously (Kondo et al., 1994). Preimmune rabbit IgG was used for the first antibody as a control. The tissues were incubated with diluted primary antibodies (4 μg/ml), and then incubated with rhodamine-conjugated goat anti–rabbit immunoglobulins (Cappel Laboratories, Cochranville, PA). After the coverslips were mounted, they were observed with a confocal laser scanning microscope (model LSM410; Carl Zeiss, Inc., Thornwood, NY).

Primary neuron cultures were prepared from hippocampi of 18-d-old fetal rats as described by Banker and Cowan (1977) and Niclas et al. (1994), with a slight modification. The cultured neurons were processed for immunofluorescence microscopy, as described previously (Kondo et al., 1994).

Ligation of Mouse Peripheral Nerves

Sciatic nerves of anesthetized 4-wk-old mice were tightly ligated under anesthesia. After 6 h, the mice were transcardially perfused with fixative as described previously (Hirokawa et al., 1990). Small pieces of nerves, both proximal and distal to the ligated portions, were frozen and sectioned on a cryostat (4–5 μm). Sections were stained using anti-KIF3B antibody (4 μg/ml) and rhodamine-labeled secondary antibody. Sections from proximal and distal regions were treated similarly and photographed with a fluorescence microscope (Axiophot; Carl Zeiss, Inc.) and printed at the same condition.

Immunoprecipitation

Brains (cerebrum) or testes of 8-wk-old male mice were homogenized by a teflon homogenizer in 10 vol of TBS (containing 1 mM EDTA and protease inhibitor mixtures). The homogenates were centrifuged at 800 g for 10 min. The supernatant was collected and NP-40 (final concentration 1%) was added. After incubation at 4°C for 30 min, the samples were centrifuged at 10,000 g for 30 min. To reduce the nonspecific binding, protein A–Sepharose (Pharmacia Inc.) was preincubated with the samples and centrifuged. Afterwards, affinity antibody (final 1 μg/ml of sample) was added to the supernatant, and the samples were incubated at 4°C for 1 h. Preimmune rabbit IgG was used as a control. The immunocomplexes were subsequently recovered on protein A–Sepharose at 4°C for 1 h. The immunocomplex-loaded beads were washed with TBS containing EDTA and protease inhibitors. Immunocomplexes were eluted with SDS sample buffer and analyzed by SDS-PAGE and silver staining. In addition, the SDS-PAGE gels were transferred to immobilon membrane, and Western blotting was performed.

In Vitro Reconstruction of the KIF3A/B Complex

To obtain the KIF3A/B complex, coinfection of both recombinant bacu-

loviruses (KIF3A and KIF3B) was conducted. It should be noted that the recombinant KIF3A virus (Kondo et al., 1994) does not contain the polyhistidine tag. Sf9 cells were infected with both viruses at ~5 multiplicity of infection. About 60 h later, cells were harvested, homogenized in Tris-HCl buffer (50 mM, pH 7.5), and centrifuged at 100,000 g for 45 min. The supernatant was added to 1/8 vol of 8× binding buffer, applied to the chelating Sepharose FF column, and eluted in PEM buffer containing 50 mM of EDTA. As a control, the same procedure was performed using only KIF3A virus. The samples were subjected to 7.5% SDS-PAGE gels, and the resultant gel was stained with Coomassie brilliant blue. The sample obtained by this procedure was used for EM and the in vitro motility assay. The molar ratio of KIF3A and KIF3B was measured by densitometry (model CS9000; Shimazu, Kyoto, Japan).

Low-Angle Rotary-shadowing EM

The purified KIF3A/B complex solutions (final protein concentration 0.025 mg/ml) were processeed for rotary-shadowing EM, as described by Hirokawa et al. (1989).

In Vitro Motility Assay and Antibody Inhibition Assay of the KIF3A/B Complex

The motility assay was performed using recombinant KIF3A/B (0.2 mg/ml) as described previously (Vale et al., 1985b; Kondo et al., 1994). Salt-extracted *Chlamydomonas* axonemes (at an appropriate concentration) (Paschal and Valee, 1993) were also used to determine the motility direction produced by KIF3A/B.

To perform antibody inhibition of the motility of the KIF3A/B complex, various concentrations of affinity-purified antibody against KIF3B were added after incubation of KIF3A/B on coverslips. After this, taxol (supplied by Dr. N. R. Lomax, National Cancer Institute), ATP, and microtubules were applied, and the movement of microtubules was observed.

Construction of the Chimeric Proteins and Truncated KIF3

We have made the following four mutant KIF3 constructs for baculovirus expression. The plasmids pBS-chimera 1 and pBS-chimera 2 were constructed in pBluescript II SK(+). To generate the pBS-chimera 1 or 2, we used the PCR method with Pfu DNA polymerase (Stratagene Inc., La Jolla, CA). Chimera 1 consists of 1–308 amino acid residues of KIF3B and 314–701 of KIF3A. Chimera 2 consists of 1–359 of KIF3B and 365–701 of KIF3A. The inserts were introduced into pBacPAK8.

To make a construct that expresses a headless 3A protein (short 3A), the full length of KIF3A plasmid was digested with PstI and EcoRI, and then the fragment of rod and tail region (nucleic acid 919-2,159) was introduced into pBacPAK8 to generate pBacPAK8/short 3A. Truncated KIF3B (amino acid 1-357), which contains only the head domain of KIF3B, was made by EcoRI digestion of full-length KIF3B and was added to the polyhistidine tag. Transfection and selection of recombinant viruses were performed as described before.

Chimera 1, chimera 2, and short 3A virus, all of which do not contain the polyhistidine tag, were then coinfected with KIF3B virus containing the polyhistidine tag. 3 d later, the cells were harvested. The proteins were extracted in binding buffer and purified by chelating Sepharose FF column. Purified proteins were used for in vitro motility assay as described above.

Subcellular Fractionation of the KIF3 Complex

40 samples of murine brain tissue (cerebrums of 7–8-wk postnatal mice) were used for subcellular fractionation as described by Kondo et al.(1994). In this procedure, the low- (P1), medium- (P2), and high- (P3) speed pellets and supernatant sample (S1, S2, and S3) were obtained. The effect of salt extraction was examined by homogenizing the P2 and P3 fractions with 0.5 M NaCl in 0.32 M sucrose buffer. These salt-extracted homogenates were centrifuged at the same speeds, and the resultant pellets (washed P2 [wP2] and washed P3 [wP3]) were analyzed by immunoblotting. P1-P3, S1-S3, and wP2/wP3 (30 μg each) were subjected to electrophoresis and transferred to an immobilon membrane. Fractions were analyzed by immunoblotting with three kinds of polyclonal antibodies (anti-KIF3A, anti-KIF3B, or anti-P38). The antibody against P38 was obtained using the following polypeptide as an antigen: SDVKMATDPENI-

IKG, corresponding to rat P38, amino acids 160–174 (Johnston et al., 1989). The relative amount of KIF3A or KIF3B in P2, P3, wP2, and wP3 was estimated by densitometry as described previously.

Further fractionation was performed to obtain the synaptic vesicle fraction. P2 was washed once in sucrose buffer and centrifuged at the same speed (P2′), and then this P2′ fraction was resuspended in 9 vol of ice-cold water. After homogenization, the resulting P2′ lysate (L) was added to Hepes-NaOH buffer (pH 7.2) (final concentration 7.5 mM) and incubated on ice for 30 min. Next, it was centrifuged for 20 min at 25,000 g to yield a lysate pellet (LP1) and a lysate supernatant (LS1). LS1 was collected and centrifuged for 2 h at 165,000 g, giving another lysate pellet (LP2) and supernatant (LS2). Subsequently, LP2 was resuspended in a total of 5 ml of 50 mM sucrose. To augment the resuspension process, the suspension was homogenized by a glass–teflon homogenizer and passed through 25- and 27-gauge needles attached to a syringe. The suspension was centrifuged at 64,700 g for 2 h on a discontinuous sucrose density gradient to give seven synaptic vesicle fractions. Synaptic vesicle fraction 1 (F1) was supernatant, fraction 3 (F3) was in 0.4 M sucrose, fraction 5 (F5) was in 0.6 M sucrose, and fraction 7 (F7) was a pellet. F2, F4, and F6 scarcely contained any material. The synaptic vesicles were most abundant in F3. P2′, LP1, LP2, F1, F3, and F7 were added to NP-40, and their protein concentration was measured by the BCA method. These samples (30 μg each) were immunoblotted with the anti-KIF3B and anti-P38 antibodies.

Isolation of Axonally Transported Organelles from Cauda Equina and Immunoisolation of Membrane-associated KIF3A/B

Axonally transported organelles in cauda equina were collected by the method described previously (Okada et al., 1995a,b). The fraction of these organelles (S2) was used for immunoisolation. Antibody against KIF3B was absorbed on protein A–Sepharose FF (Pharmacia Inc.), and was covalently cross-linked by dimethylpimelimidate. S2 was incubated with the beads, and the beads were recovered by centrifugation and washed with internal medium. Preimmune rabbit IgG was used for control studies. The beads were processed for conventional EM and observed as described previously (Noda et al., 1995).

Gel Filtration Assay

The molecular size of the native KIF3 complex and recombinant KIF3A/B were estimated by gel filtration on a Superose 6 column (Pharmacia Inc.), followed by subsequent immunoblotting with the antibody against KIF3A and KIF3B. Brain or testes of 9-wk-old male mice were homogenized in 3 vol of TBS (containing 1 mM EDTA and protease inhibitors). The homogenates were centrifuged at 800 g for 10 min. The supernatant was collected and NP-40 (final concentration 1%) was added. After incubation at 4°C for 30 min, 1 ml of samples was centrifuged at 100,000 g for 45 min and loaded on the column. Purified recombinant KIF3A/B (80 μg) was also centrifuged at the same speed and loaded. The fractions were then collected, and Western blotting was performed to determine the peak fraction. Calibration was performed with standard proteins (gel filtration calibration kit; Pharmacia Inc.) according to the manufacturer's instructions.

Results

Primary Structure of KIF3B Revealed a Great Similarity with KIF3A

We previously reported five new members of the kinesin superfamily found in the murine central nervous system (Aizawa et al., 1992). To find additional members in this superfamily, PCR was performed using degenerate primers corresponding to the ATP- and microtubule-binding domains conserved in the kinesin superfamily. In this experiment, we found a new clone that was homologous to KIF3A (formerly designated KIF3), but not identical to it. Thus, we named this clone KIF3B, and renamed KIF3 as KIF3A.

To examine the structure of KIF3B in detail, we screened KIF3B cDNA, obtained from the 0-d-old murine brain

cDNA library, using a PCR-amplified cDNA fragment of KIF3B as a probe. Nucleotide sequence analysis revealed the presence of a single open reading frame of 2,241 nucleotides that encoded 747–amino acid residues (M_r, 85,281; Fig. 1 A). According to the Chou-Fasman (Chou and Fasman, 1974) and Robson-Garnier (Robson and Suzuki, 1976; Garnier et al., 1978) secondary structure prediction method (Mac vector DNA analysis software International Biotechnologies, Inc., New Haven, CT), KIF3B has an NH_2-terminal domain (head globular domain, amino acid residues 1–363), a central domain (rod α-helix domain, amino acid residues 364–592), and a COOH-terminal domain (tail globular domain, amino acid residues 593–747) (Fig. 1 C). A diagonal dot matrix comparison of KIF3A

and KIF3B showed high similarity exists in the head domain (including motor domain) and the latter half of the rod domain (Fig. 1 B). Among all the murine kinesin superfamily proteins sequenced thus far, KIF3B has the highest identity with KIF3A (47% in overall length and 69% in the motor domain; amino acid residues from IFAFGQT to VDLAGSE).

Northern blot analysis was performed to compare their respective expression in developing neurons and various tissues (Fig. 2 A). We used the rod domain cDNA fragments as probes, and neither probe showed cross-hybridization. The KIF3B transcript is a single band of 5.5 kbp, whereas KIF3A has transcripts of 5.3, 4.0, and 2.5 kbp. To examine their expression in developing neurons, we used
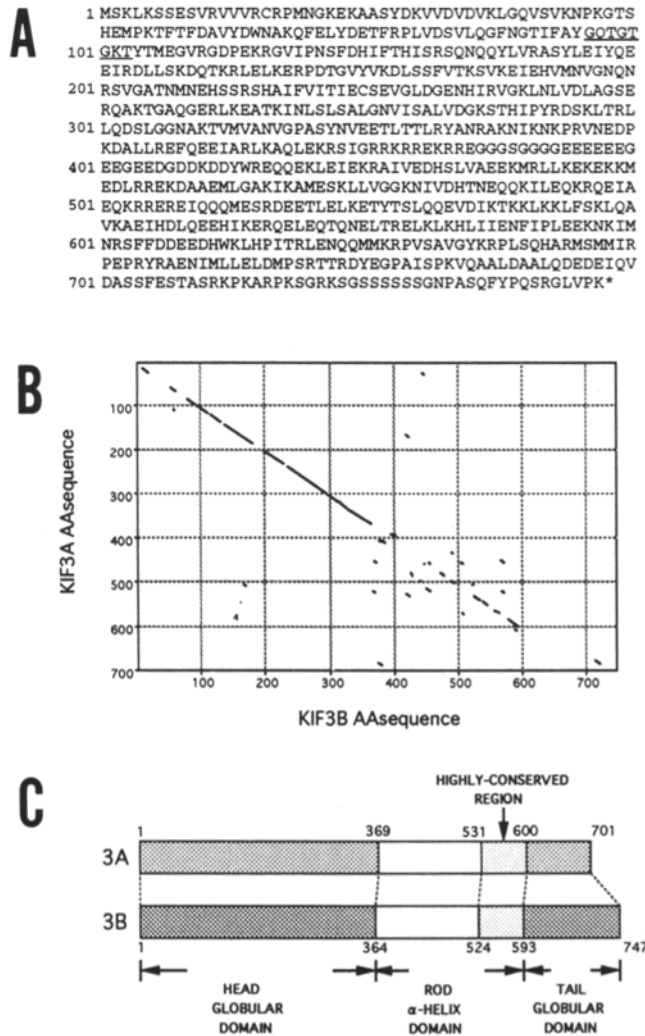

A

```
  1 MSKLKSSESVRVVVRCRPMNGKEKAASYDKVVDVDVKLGQVSVKNPKGTS
    HEMPKTFTFDAVYDWNAKQFELYDETFRPLVDSVLQGFNGTIFAY GQTGT
101 GKTYTMEGVRGDPEKRGVIPNSFDHIFTHISRSQNQQYLVRASYLEIYQE
    EIRDLLSKDQTKRLELKERPDTGVYVKDLSSFVTKSVKEIEHVMNVGNQN
201 RSVGATNMNEHSSRSHAIFVITIECSEVGLDGENHIRVGKLNLVDLAGSE
    RQAKTGAQGERLKEATKINLSLSALGNVISALVDGKSTHIPYRDSKLTRL
301 LQDSLGGNAKTVMVANVGPASYNVEETLTTLRYANRAKNIKNKPRVNEDP
    KDALLREFQEEIARLKAQLEKRSIGRRKRREKRREGGGSGGGGEEEEEEG
401 EEGEEDGDDKDDYWREQQEKLEIBKRAIVEDHSLVAEEKMRLLKEKEKKM
    EDLRREKDAAEMLGAKIKAMESKLLVGGKNIVDHTNEQQKILEQKRQEIA
501 EQKRREREIQQQMESRDEETLELKETYTSLQQEVDIKTKKLKKLFSKLQA
    VKAEIHDLQEEHIKERQELEQTQNELTRELKLKHLIIENFIPLEEKNKIM
601 NRSFFDDEEDHWKLHPITRLENQQMMKRPVSAVGYKRPLSQHARMSMMIR
    PEPRYRAENIMLLELDMPSRTTRDYEGPAISPKVQAALDAALQDEDEIQV
701 DASSFESTASRKPKARPKSGRKSGSSSSSSGNPASQFYPQSRGLVPK*
```

B

KIF3A AAsequence (y-axis, 100–700)

KIF3B AAsequence (x-axis, 100–700)

C

HIGHLY-CONSERVED REGION

```
        1              369    531 ↓600      701
  3A    [                                      ]
        1              364    524 593        747
  3B    [                                      ]

        ←  HEAD       → ←  ROD  → ← TAIL →
           GLOBULAR       α-HELIX    GLOBULAR
           DOMAIN         DOMAIN     DOMAIN
```

Figure 1. (A) Amino acid sequences (single-letter code) of KIF3B. The putative ATP-binding site in the motor domain is underlined. These sequence data are available from GenBank/ EMBL/DDBJ Data Library under accession number D26077. (B) Sequence comparison between KIF3A and KIF3B. Diagonal dot matrix comparisons were performed on MacVector DNA analysis software using a window size of 8 and stringency of 60%. AA, amino acid. (C) Diagram showing the secondary structure predictions of KIF3A and KIF3B. Predictions were performed by the Chou-Fasman and Robson-Garnier methods using the above software.
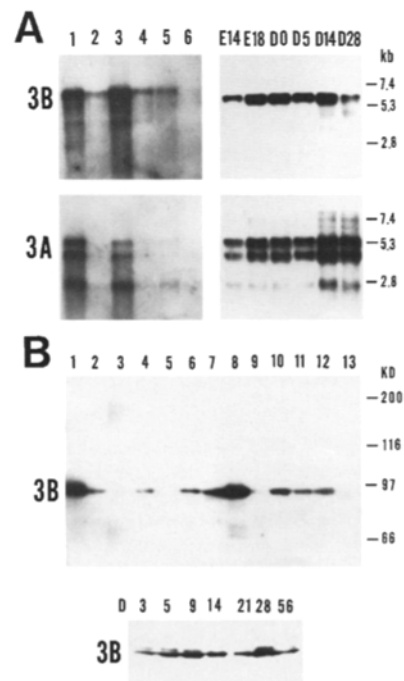
Figure 2. (A) Northern blot analysis of the KIF3A and KIF3B transcripts (*upper panels*, KIF3B; *lower panels*, KIF3A). (*Left*) KIF3A and KIF3B expression in different mouse tissues. Abundant transcripts of KIF3A and KIF3B can be seen in brain and kidney tissues. Samples (~1 μg) of mRNA from various tissues were loaded: brain (lane *1*), liver (lane *2*), kidney (lane *3*), lung (lane *4*), spleen (lane *5*), heart (lane *6*). (*Right*) Developmental profiles of KIF3A and KIF3B expression. The expression patterns showed slight differences between them. mRNA (2 μg) from embryo and postnatal mouse brains was loaded and electrophoresed. *E*, embryo age in days; *D*, postnatal age in days. (*B*) Western blot analysis of KIF3B. (*Upper panel*) Expression of KIF3B in various tissues. Samples were crude extracts (1 μl on each lane) of tissues from 8-wk-old mice. The antibody only recognizes KIF3B, and no cross-reactions are present. Cerebrum (lane *1*), spleen (lane *2*), liver (lane *3*), kidney (lane *4*), heart (lane *5*), lung (lane *6*), small intestine (lane *7*), testis (lane *8*), ovary (lane *9*), pancreas (lane *10*), adrenal gland (lane *11*), thymus (lane *12*), and skeletal muscle (lane *13*). Molecular weights are as indicated. KIF3B is strongly expressed in cerebrum and testis. (*Lower panel*) Expression of KIF3B in developing neurons. No change is apparent in expression of KIF3B. Age of postnatal mice is indicated in days (*D*) above each lane.

mouse embryos at days 14 and 18, as well as postnatal animals at days 0, 5, 14, and 28. Results indicate that the amount of expression of transcripts did not significantly change during development, although their expression patterns showed a slight difference at day 28. Distribution of KIF3A and KIF3B mRNA in brain, liver, kidney, lung, spleen, and heart tissues of day 14 mice showed both transcripts to be highly expressed in the brain and kidney, but only weakly expressed in the other tissues. Note that the expression patterns of KIF3A and KIF3B show a distinct resemblance.

Recombinant KIF3B Can Be Purified by the Polyhistidine Tag Method

To characterize the properties of KIF3B, we expressed it using the baculovirus-Sf9 expression system described by O'Reilly et al. (1992). Purification of the resultant recombinant KIF3B protein expressed in the Sf9 cells was carried out by constructing a modified KIF3B cDNA that includes a polyhistidine tag in the COOH terminus. Recombinant KIF3B protein was purified by a chelating Sepharose FF column (nickel column). Approximately 90% of the KIF3B protein was found to be soluble at a high salt concentration (binding buffer or elution buffer; see Materials and Methods) having a purity >95%, whereas it was not recovered in soluble fractions when the cells were homogenized in a low-salt buffer (~100 mM salt). Also, purified KIF3B aggregated when it was dialyzed against buffers at physiological ionic strength. When recombinant KIF3B was expressed without the polyhistidine tag, a similar tendency was found (data not shown), thereby suggesting that KIF3B is not stable under physiological conditions.

Using the purified KIF3B protein as an antigen, we raised a polyclonal antibody against KIF3B, and then affinity purified it by an activated Thiol–Sepharose 4B affinity column (Pharmacia Inc.). The resultant antibody specifically reacted with the KIF3B protein (both baculovirus-expressed KIF3B and mouse brain KIF3B), but did not cross-react with KIF3A or other KIFs (Fig. 2 B).

KIF3B Is Associated with an Anterograde-moving Organelle That Is Transported by Fast Axonal Flow

To investigate KIF3B's expression in tissues and developmental neurons, and to examine the difference between KIF3A and KIF3B, we performed Western blot analysis on various organs of 8-wk-old mice and developing brains (Fig. 2 B). The affinity-purified polyclonal antibody was used against KIF3B, which strongly expressed in the brain and testes. In the other organs, however (i.e., spleen, liver, kidney, lung, intestine, ovary, pancreas, adrenal gland, and thymus), KIF3B was only weakly expressed, while expression in the heart and skeletal muscle was barely detected.

Expression in various parts of the nervous system (cerebrum, cerebellum, hippocampus, spinal cord, and sciatic nerve) was also examined, and KIF3B was most strongly expressed in the hippocampus and least so in the sciatic nerve (data not shown). Although KIF3B's immunoreactive band was also detected as a doublet in the central nervous system tissues, the upper band was weak and frequently could not be detected. The developing cerebrum

in 3-d- to 8-wk-old mice was examined by immunoblotting, with KIF3B showing no remarkable change in expression during development. These results with KIF3B are almost identical to those found with KIF3A (data not shown).

We also examined KIF3B localization in nerve tissues by immunofluorescence microscopy (Fig. 3 A). In the cerebrum, cerebellum, and hippocampus of 8-wk-old mice, anti-KIF3B antibody strongly stained the cell bodies of most neuronal cells. Axons and dendrites were also stained, though somewhat more weakly compared with the cell bodies.

To obtain more information on the subcellular distribution of KIF3B, immunostaining was performed in cultured embryonic hippocampal neurons (data not shown). KIF3B was localized mainly in cell bodies. Axons and dendrites were also stained, though somewhat more weakly compared with the cell bodies. Collectively, KIF3B was mainly localized in neurons, fairly so in the cell bodies, and to a lesser degree in the axons and dendrites.

Next, our previous studies demonstrated the presence of anterograde- and retrograde-moving membranous organelles being transported by fast axonal flow; these organelles accumulate at the proximal and distal portions of axons, respectively, ~6 h after ligation of mouse peripheral nerves (Hirokawa et al., 1990, 1991). Thus, the proximal and distal portions of ligated sciatic nerves were stained with the anti-KIF3B antibody. Immunofluorescence microscopy subsequently revealed that the anti-KIF3B antibody strongly and reproducibly stained nerve regions proximal to the ligation. Contrastingly, staining in regions distal to the ligated parts was comparatively weak, as shown in Fig. 3 B. These results indicate that peripheral nerve axons contain a particular amount of KIF3B, and it anterogradely accumulates at a ligation. The results with KIF3B are also identical to those found with KIF3A (Kondo et al., 1994). We consequently believe this protein is strongly associated with anterograde-moving organelles that are transported by fast axonal flow in vivo.

KIF3A and KIF3B Are Components of the KIF3 Complex In Vivo

Our results clearly indicate that KIF3A and KIF3B may be associated with each other; that is, they showed a similar expression pattern in the central nervous tissues and other organs, Western blot analysis produced similar results, and similarities occurred in their immunological localization and in the peripheral nerve ligation experiment.

To examine this possibility, we performed immunoprecipitation by anti-KIF3A and anti-KIF3B antibodies in mouse brain extracts, with several bands (80/85, 95, 100–105 kD) being precipitated by both antibodies. The 80/85 and 95 kD bands, respectively, correspond to the molecular weight of KIF3A and KIF3B, and from 100 to 105 kD, three bands were consistently precipitated by both antibodies (Fig. 4 A, lanes 1 and 2). To characterize these bands, immunoblotting analysis was carried out on their gels (Fig. 4 A, lanes 4–9). In both filters, the bands at 80/85 kD were stained by anti-KIF3A (lanes 7 and 8), and that at 95 kD was stained by anti-KIF3B (lanes 4 and 5). However, the bands from 100 to 105 kD were not stained by these antibodies. These results indicate that KIF3A and
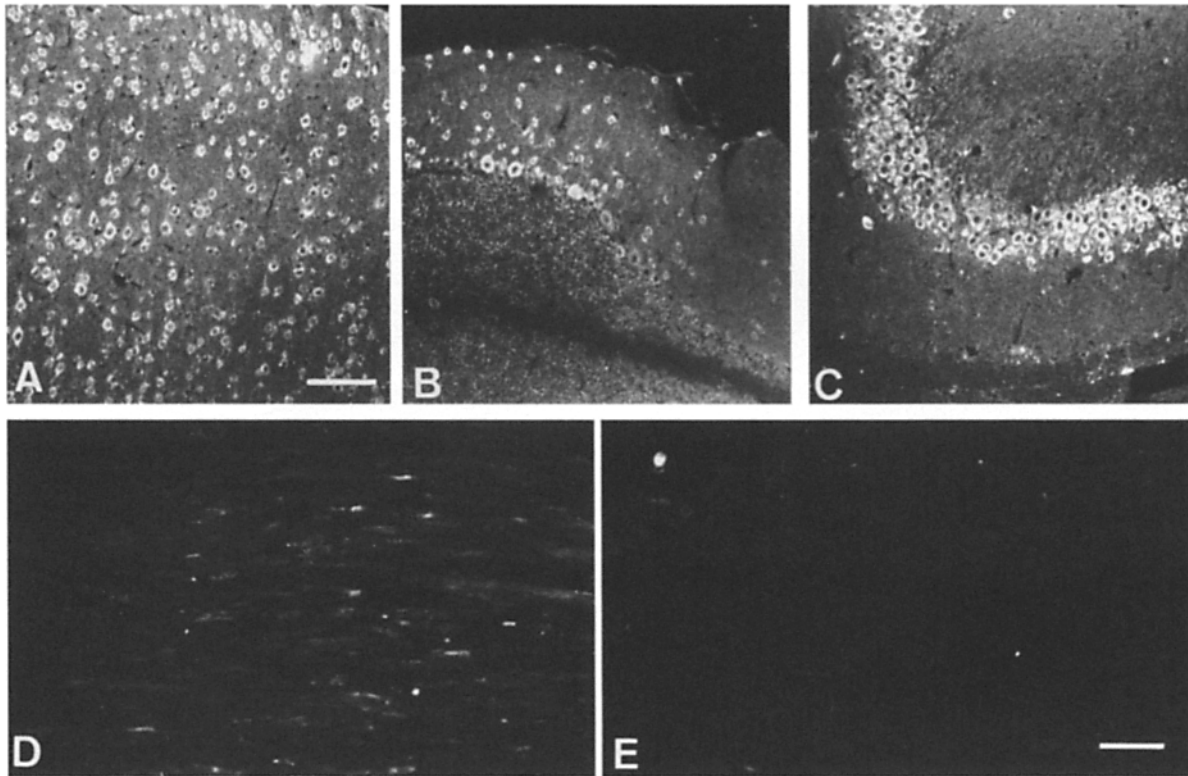
Figure 3. (*A–C*) Immunofluorescence micrographs of 8-wk-old mouse cerebrum (*A*), cerebellum (*B*), and hippocampus (*C*) stained with anti-KIF3B antibodies. The cell bodies of neurons are strongly stained with KIF3B antibodies, while dendrites and axons show lower intensity. (*D* and *E*) Immunofluorescence micrographs of sections of ligated mouse sciatic nerves stained with anti-KIF3B antibodies proximal (*D*) and distal (*E*) to the ligations. The ligated portion is between these figures, 0.1 mm from each of them. Anti-KIF3B antibodies strongly stained the proximal portions, whereas the distal portions show less intensity. Bars, 50 μm.

KIF3B coprecipitated with the anti-KIF3B antibody and also with the anti-KIF3A antibody, and that the three upper bands may be proteins associated with both proteins. Taken together, KIF3A and KIF3B obviously form a complex that probably contains new, high-molecular weight "associated proteins." We named these associated proteins kinesin superfamily–associated protein 3 (KAP3).

We also carried out the same immunoprecipitation measurements on tissue from mouse testis, where it was found that KAP3 only had a single band (Fig. 4 *B*) vs the three bands in brain tissue, as well as having a different height. This observation suggests that composition of these associated proteins may vary in various cell types.

KIF3A and KIF3B Form a Heterodimer In Vitro That Provides Plus End–directed Motor Activity

A question of interest is why do KIF3A and KIF3B and their associated proteins form a complex in vivo. One possibility is their mutual association, while another is that KIF3A and KIF3B only associate with themselves. To test these, we performed an in vitro reconstruction experiment in Sf9 cells by coinfecting them with the KIF3A and KIF3B recombinant virus; the former virus (Kondo et al., 1994) has no polyhistidine tag. As controls, cells infected with only KIF3A virus were also prepared and purified by the same procedure. After infection, the cells were harvested, and the proteins were purified by the polyhistidine tag method. Coomassie brilliant blue staining revealed two

bands on the lane of the coinfected sample. The lower band was the same height as KIF3A's, the upper band was the same height as KIF3B's, and the densitometry assay revealed that their molar ratio was about 1:1 (Fig. 5 *A*, lane *7*). We then used immunoblotting to confirm that both bands were KIF3A and KIF3B (Fig. 5 *B*, lanes *2* and *4*). In the cells infected with KIF3A virus alone, the expression of KIF3A was seen in the crude homogenate (lane *2*), but no protein was purified by this method (lane *5*), that is, the method enabled KIF3A to be copurified using the Sf9 cells coinfected with KIF3A and the KIF3B–polyhistidine tag virus. Based on these results, recombinant KIF3A and KIF3B directly form a complex in vitro; hence the presence of the associated proteins is probably not essential in forming this complex.

The molecular structure of the recombinant KIF3A/B complex was analyzed by low-angle rotary-shadowing EM (Fig. 6). Because purification with the polyhistidine tag method recovers KIF3B monomer and the KIF3A/B complex, we purified the complex by taking advantage of the fact that the monomer aggregates in a low-salt buffer. Extraction of coinfected Sf9 cells with this buffer separates the complex as a supernatant from the monomer aggregates. KIF3A/B in the supernatant was then highly purified using the polyhistidine tag (Fig. 5 *A*). The rotary-shadowed complex exhibited a number of consistent morphological features with the heterodimerization of KIF3A and KIF3B. For instance, most of the molecules had a rod-
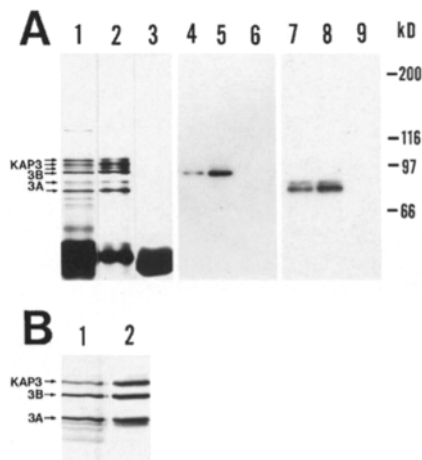
Figure 4. (A) Immunoprecipitation of KIF3A and KIF3B from mouse brain extracts. Lanes 1–3 show silver staining of immunoprecipitates in SDS-PAGE gel: immunoprecipitation by anti-KIF3A antibody (lane 1); immunoprecipitation by anti-KIF3B antibody (lane 2); control preimmune rabbit IgG (lane 3); Western blotting of the gel of lanes 1–3 (lanes 4–9); anti-KIF3B antibody staining (lanes 4–6); anti-KIF3A antibody staining (lanes 7–9). In addition to the immunoglobulin bands (~40 kD), several bands were consistently observed (lanes 1 and 2). The 80/85-kD band is KIF3A (lanes 7 and 8) and that of 95 kD is KIF3B (lanes 4 and 5). Three bands of associated proteins (KAP3) (100–105 kD) are apparent in both precipitations (lanes 1 and 2). In the control lane, only immunoglobulin is present (lane 3). (B) Silver staining of immunoprecipitation by anti-KIF3A and anti-KIF3B antibody from the testis. Only a single band of KAP3 (it is almost the same height with the middle band in the brain) is shown in the testis. Lane 1 shows immunoprecipitation by anti-KIF3A antibody; lane 2 shows immunoprecipitation by anti-KIF3B antibody. Note that the molar ratio of KIF3A, KIF3B, and KAP3 in the testis was approximately 1:1:0.7.

Figure 5. In vitro reconstruction of the KIF3A/B complex. (A) Coomassie brilliant blue staining of the gel. Lane 1 shows 8-wk-old mouse brain homogenates. Lanes 2–4 show crude extracts of baculovirus-expressed Sf9 cell proteins. Lane 2 shows infection with KIF3A recombinant virus; lane 3 shows infection with KIF3B recombinant virus; and lane 4 shows coinfection with recombinant KIF3A and KIF3B viruses. Lanes 5–7 show proteins purified by the polyhistidine tag method from Sf9 cells infected with KIF3A virus (lane 5), KIF3B virus (lane 6), or KIF3A/B virus (lane 7). Lane 8 shows control KIF3A purified by the microtubule-binding method (Kondo et al., 1994). KIF3A was not purified by the polyhistidine tag method using homogenates of Sf9 cells expressing only KIF3A because recombinant KIF3A does not contain this tag (lane 5). However, KIF3A was copurified from the homogenates of Sf9 cells coinfected with the KIF3A and the KIF3B–polyhistidine tag virus by the polyhistidine tag method (lane 7). Lefthand lane is the molecular weight marker. (B) Western blot analysis of 8-wk-old mice brain homogenates and purified baculovirus-expressed KIF3A/B complex. Lanes 1 and 3 show brain homogenates; lanes 2 and 4 show purified KIF3A/B complex; lanes 1 and 2 show staining with anti-KIF3B antibody; and lanes 3 and 4 show staining with anti-KIF3A antibody. The molecular weight of recombinant KIF3A coincides with the 85-kD band of native KIF3A.

shaped configuration with a length of ~50 nm (48.8 ± 3.1 nm, n = 120). One end of the molecule typically displayed two globular structures, referred to as the head (long diameter of head 10.4 ± 1.0 nm, n = 60), while a small globular structure was located at the tail end of the molecule. The head and tail regions were connected by a straight, short shaft. In comparison with bovine brain kinesin (Hirokawa et al., 1989), the KIF3A/B complex has a similar head domain structure with a short rod domain. KIF3A has nearly the same length and long diameter of head as KIF3A/B, but in contrast, it usually has a single head and a thin rod region (Kondo et al., 1994). These findings suggest that KIF3A and KIF3B form a heterodimer consisting of a single molecule of KIF3A and KIF3B.

Next, to confirm that the complex is a microtubule-based motor protein, we performed an in vitro motility assay of microtubules and Chlamydomonas axonemes (Fig. 7). We performed an in vitro motility assay using the purified KIF3A/B complex. It showed plus end–directed motor activity, induced microtubule motility at ~0.3 μm/s (n = 20), and moved all of the axonemes toward their minus ends (n = 69) at almost the same velocity.

Since we did not purify KIF3A/B using usual procedures for purifying motor proteins, for example, nucleotide-dependent microtubule binding, its transport activity is al-
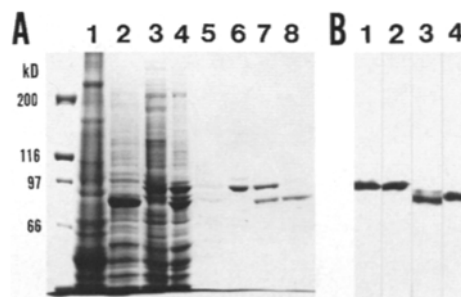
most surely not due to low-level contamination with an unknown motor protein. To further eliminate this limited possibility, as well as to investigate the effect of the anti-KIF3B antibody on the motility of KIF3A/B, we performed an antibody inhibition assay for microtubule motility (Fig. 8). We used preimmune rabbit IgG as a control, and motility was not subsequently affected by it. We found that as the concentration of the anti-KIF3B antibody increased, a decrease occurred in: (a) the number of microtubules that were attached to the glass surface; and (b) the proportion of moving microtubules (Table I). Interestingly, the velocity of microtubules decreased as the concentration of the antibody increased, until at 0.2 mg/ml, microtubules on the glass were scarcely seen, and all the microtubules attached to the glass remained stationary. These results indicate that the KIF3A/B complex possesses motor activity and that an antibody against KIF3B

Table I. Antibody Inhibition Assay of KIF3A/B Complex Motility in Vivo

Antibody concentration (mg/ml)	0	0.005	0.017	0.05	0.2	Normal IgG
Motility (%)*	100	80	70	55	0	100

*The motility of microtubules was determined by the ratio of motile microtubules to total microtubules bound on coverslips. At each concentration, 20 microtubules were examined.
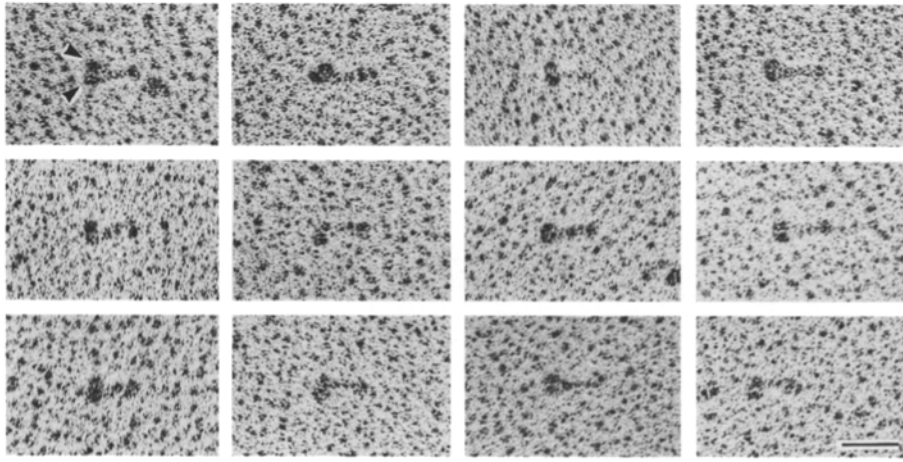
Figure 6. Low-angle rotary-shadowing electronmicrographs of recombinant KIF3A/B complex. Single molecule of the recombinant KIF3A/B complex. Several representative molecules are indicated. Arrowheads indicate the heads. Note the number of heads (*arrowheads*). In the tail domain of KIF3A/B, a small globular structure appears. Bar, 50 nm.

affects KIF3A/B by blocking microtubule sliding and microtubule-binding activity.

KIF3B Head Has Motor Activity as Well as KIF3A

In the present study, we showed that KIF3A/B heterodimer also has motor activity in vitro. We have already shown that KIF3A itself is sufficient for supporting microtubule motility in vitro (Kondo et al., 1994). Then a question arises whether KIF3B itself is sufficient to induce microtubule motility or if it only modifies the motor activity of KIF3A. We have tried the in vitro motility assay using a full length of KIF3B. Although several experiments were performed in various conditions, we could not show its motility because of aggregation. A truncated KIF3B construct (amino acid 1–357) was made and expressed by the baculovirus system, but it also aggregated in the same conditions. To overcome this problem, we tried to take advantage of the fact that KIF3B is solubilized by making a complex with KIF3A in the rod–tail domain. We designed a protein complex that has two KIF3B heads by replacing a head domain of KIF3A to that of KIF3B, or a protein complex that has only one motor domain by deleting the head domain of KIF3A, leaving the KIF3B polypeptide intact. In either case, if microtubule motility is shown, then the KIF3B head domain is proven to have motor activity, because the KIF3A head is not included in these complexes. For this purpose, we constructed three altered virus vectors (chimera 1, chimera 2, and short 3A) by PCR, and each of them was coinfected with a full length of KIF3B virus containing the polyhistidine tag to perform an in vitro motility assay using microtubules or *Chlamydomonas* axonemes. Chimeras 1 and 2 have a KIF3B head (amino acid 1–308)/KIF3A rod tail (amino acid 314–701), and a KIF3B head (amino acid 1–359)/KIF3A rod tail (amino acid 365–701), respectively. On the other hand, short 3A consists of only a rod–tail region (amino acid 317–701). All the proteins do not contain a polyhistidine tag, so if they form a complex with each other, we can copurify each altered protein with KIF3B protein by nickel column. The results are shown in Fig. 9, indicating the complex formation and motility assay with the schema of constructs. Short 3A aggregated in physiological conditions so that it did not form a complex. Chimera 1 and chi-

mera 2 are soluble, and both of them formed a complex with KIF3B in vitro. Interestingly, chimera 1 showed plus end–directed microtubule motility at $\sim$0.3 μm/s ($n = 20$), whereas we could not show the motility of chimera 2 in any conditions (though it revealed microtubule-binding activity). These results indicate that the KIF3B head itself can reveal motor activity even if its rod–tail region is KIF3A's. Furthermore, the structural difference between chimera 1 and chimera 2 is that the former contains KIF3A's "neck," which connects head domain and rod domain, and the latter has KIF3B's one. These opposite results in motility suggest the importance of this "neck" region to microtubule motility.

The KIF3 Complex Associates with the Membranous Organelles, but Is a Putative Nonsynaptic Vesicle Motor In Vivo

We used a centrifugation sedimentation assay of mouse brain homogenates to analyze the subcellular localization of the native KIF3A/B complex with associated proteins, called the KIF3 complex. After low-, medium-, and high-speed centrifugation (see Materials and Methods), Western blot analysis was performed on all particulate (P1–P3) and supernatant (S1–S3) fractions. Previous studies showed that the low-speed pellets (P1) contain the nuclear fraction and mitochondria, medium-speed pellets (P2) the synaptosomes and lysosomes, and high-speed pellets (P3) mostly microsomes (Ueda et al., 1979). Only P1 had relatively less of the KIF3 complex, while P2, P3, and S1–S3 showed almost the same amounts (Fig. 10 *A*). To determine whether KIF3 tightly binds to sedimented organelles, P2 and P3 were washed and extracted with 0.5 M NaCl in 0.32 M sucrose buffer (wP2 and wP3). After this, 70–80% of the complex was detached from the sedimented organelles.

The P2 fraction was further fractionated by hypoosmotic shock and sucrose gradient centrifugation to investigate whether KIF3 binds to synaptic vesicles (Fig. 10 *B*). The blot was stained with an antibody against synaptic vesicle membrane protein P38 (synaptophysin) (Huttner et al., 1983), and the peak fraction of KIF3 was clearly distinct from the peak of P38. In addition, KIF3's peak fraction was a supernatant of the sucrose density gradient
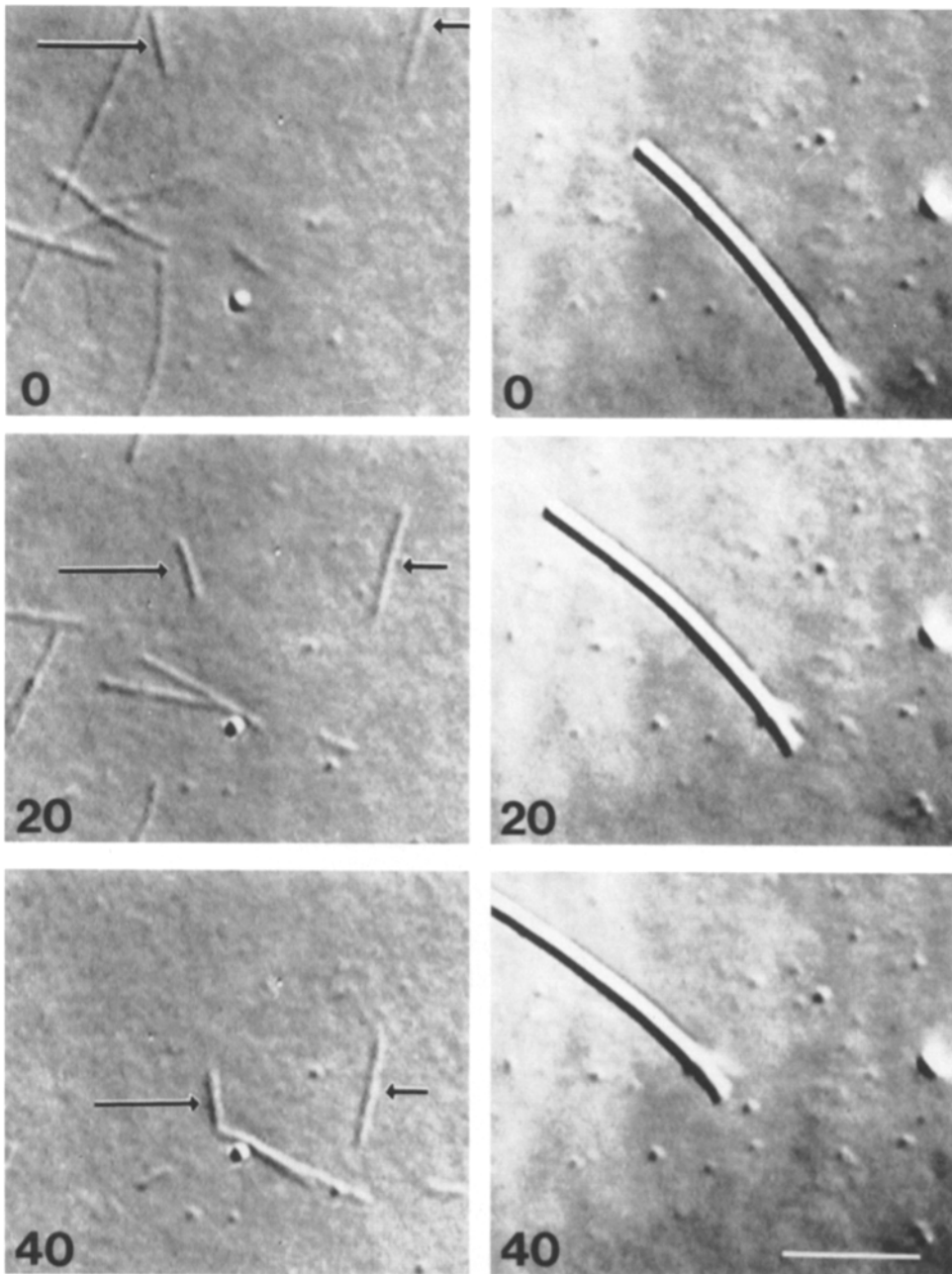
Figure 7. In vitro motility assay of polyhistidine tag–purified KIF3A/B. (*Left*) Moving microtubules taken at 20-s intervals. Arrows indicate the tips of moving microtubules. (*Right*) Analysis of the direction of the movement produced by recombinant KIF3A/B. *Chlamydomonas* axonemes were assayed for gliding activity, and they glided toward their compact end, indicating plus end–directed motility activity of KIF3A/B. Bar, 5 μm.

(F1), while the peak of P38 was in F3 (synaptic vesicle fraction; see Materials and Methods).

Thus, in subcellular components, the KIF3 complex exists in ubiquitous fractions. We could not confirm, however, that it is abundantly present in synaptic vesicle fractions.

Next, to confirm that KIF3 actually associates with the membranous organelles, membrane-associated KIF3 was isolated by immunoprecipitation with anti-KIF3B antibody–conjugated Sepharose beads. The rat cauda equina homogenates were centrifuged at low speeds. Then the supernatant was reacted with antibody-conjugated beads. EM showed various sizes of vesicles (90–160 nm diam) located on the surface of the beads (Fig. 11 *A, C–E*), while none were present on preimmune IgG-conjugated ones (Fig. 11 *B*), indicating that KIF3B immunoprecipitated in

membrane bound form. At higher magnification, vesicles are mostly 90–160 nm in diameter, but multivesicular bodies were not observed. These results support the findings that KIF3 associates with the transported membranous organelles in nerve axons.

The KIF3 Complex Is a Heterotrimeric Motor In Vivo

We measured the molecular size of the native KIF3 complex in the brain and the recombinant KIF3A/B complex using gel filtration and immunoblotting. From these experiments, we estimated the native relative molecular mass of KIF3 to be ~350 kD and recombinant KIF3A/B to be ~250 kD. The same results were also obtained for the testis.

Next, to determine the accurate molar ratio of each subunit of the native KIF3, we used gel densitometry of the
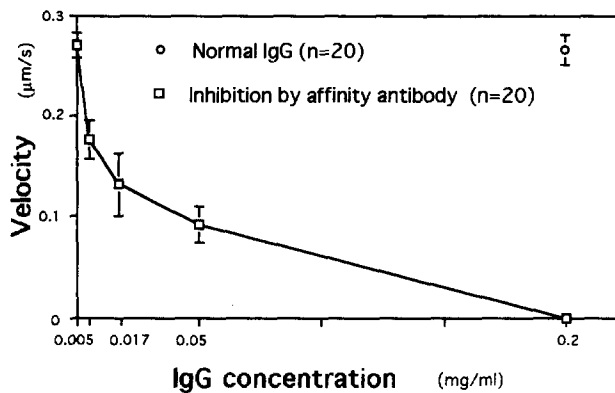
Figure 8. Antibody-blocking assay of KIF3A/B motility. The velocity of the microtubule slows as the antibody concentration increases, and finally all microtubules on the cover glass remain stationary. Preimmune IgG showed no effect on their motility.

lane containing KIF3A, KIF3B, and KAP3. As each subunit consists of a single band in the testis, we measured the immunoprecipitates of them. Silver or Coomassie brilliant blue staining of the gel revealed that the average molar ratio was KIF3A/KIF3B/KAP3 = 1:1:0.7.

Taken together with our EM data, it seems likely that most of the native KIF3 may be a heterotrimeric protein comprised of 1 mol KIF3A (80/85 kD), 1 mol KIF3B (95 kD), and 1 mol KAP3 (100–105 kD), with a total molecular mass of ~300 kD. The decrease in the molar ratio of KAP3 to the KIF3A/B heterodimer suggests that a small fraction of KIF3A/B is free of KAP3, while the majority portion is associated with a KAP3 polypeptide.

Discussion

KIF3B Forms a Heterodimer with KIF3A

Our immunoprecipitation measurements on mouse cerebrum by anti-KIF3A or anti-KIF3B antibodies both showed that KIF3A and KIF3B form a complex with KAP3 in vivo. We also proved by the in vitro reconstruction assay using the baculovirus expression system that KIF3B directly binds to KIF3A, and that KAP3 is not essential for this binding. Moreover, EM analysis revealed that the KIF3A/B complex has two globular structures (head) on one end that are connected by a short rod domain to a single globular structure (tail) at the other end, hence indicating that KIF3A and KIF3B form a heterodimer at the α-helical rod domain. This is further supported by our antibody inhibition experiment on the KIF3A/B complex. Antibody specific to KIF3B inhibited the microtubule motility by the KIF3A/B complex in vitro as shown in the present study, while KIF3A by itself produced microtubule motility in vitro (Kondo et al., 1994). These findings suggest that the motor function of the KIF3A head domain is severely affected by the presence of the antibody decoration on KIF3B, which inhibits microtubule sliding and microtubule-binding activity. This antibody decoration may either restrict the motility of the complex by producing resistance or cause a steric hindrance that prevents the KIF3A head from binding to the microtubule.

When KIF3B's amino acid sequence was compared with other predicted kinesin-related proteins by the CLUSTAL V computer program (Higgins et al., 1992), it was most similar to sea urchin KRP85K/95K (Cole et al., 1993) and *Drosophila* KLP64D/68D (Stewart et al., 1991; Pesavento et al., 1994; for review see Goldstein, 1993). By comparing the identity in the motor domain among these proteins, KIF3B was found to have 69 and 89% identity (amino acid; from IFAYGQT to VDLAGSE) with KRP85K and KRP95K, respectively, and 72 and 65% identity (fragment sequence of the motor domain) with KLP64D and KLP68D, respectively. On the other hand, KIF3A showed corresponding identities of 84 and 70% with the former proteins and 78 and 62% with the latter ones. Such identities suggest that KIF3A and KIF3B may be respective counterparts of sea urchin KRP85K and KRP95K, which were immunoprecipitated from cytosol as a complex having a 115-kD subunit (Cole et al., 1993). It is not proven whether KRP85K and KRP95K form a heterodimer, but if so, this would strongly support our findings.

The expression pattern of KIF3A and KIF3B showed good agreement in the protein level of all organ tissues subjected to Western blot analysis. However, the North-
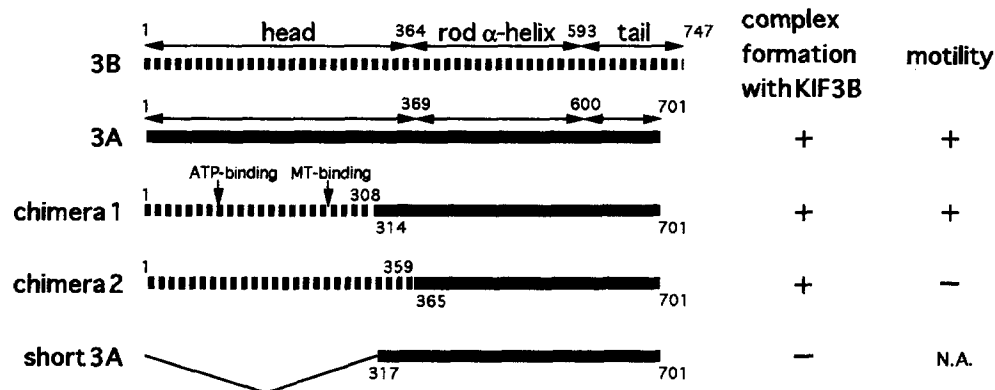

Figure 9. Summary of the results from the copurification experiments and the in vitro motility assays of various KIF3A/B constructs. Full-lengths of KIF3B and KIF3A are shown at the top. Chimera 1, chimera 2, and short KIF3A are described below. All of them, except for the full-length KIF3B, do not contain the polyhistidine tag. Domain structure (head, rod α-helix, and tail) or ATP-binding site and microtubule (*MT*)-binding site are indicated by arrows. The positions where the KIF3B head and KIF3A rod–tail are connected in chimera and where KIF3A is truncated are also described. The numbers in each protein are the amino acid positions of KIF3A and KIF3B. Each construct was coinfected with full-length KIF3B containing the polyhistidine tag and purified by nickel column. Although chimeras 1 and 2 formed a complex, only chimera 1 showed microtubule motility. Short 3A aggregated in physiological conditions and did not form a complex. *NA*, not applicable.
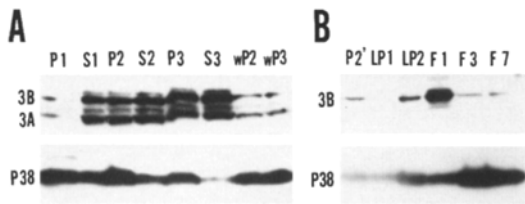
Figure 10. Subcellular localization of the KIF3 complex in vivo. (A) Immunoblot of KIF3A and KIF3B in the fractions of S1–S3, P1–P3, washed P2 (wP2) and washed P3 (wP3). The same amount of protein (30 μg) from each fraction was applied to SDS-PAGE and analyzed. P1 contains a small amount of the KIF3 complex, whereas the other fractions (S1–S3, P2, and P3) contain almost equal amounts of KIF3. wP2 and wP3 indicate that KIF3 tends to detach from the membrane components in a high-salt condition. (B) The synaptosome fraction from mouse brain was fractionated by sucrose gradient centrifugation and analyzed by immunoblotting. Anti-P38 (synaptophysin) antibody was used to detect the P38-containing vesicle fractions. Each fraction (see Materials and Methods) was stained by the anti-KIF3B and anti-P38 antibodies. The peak fraction of KIF3B is clearly distinct from that of P38.
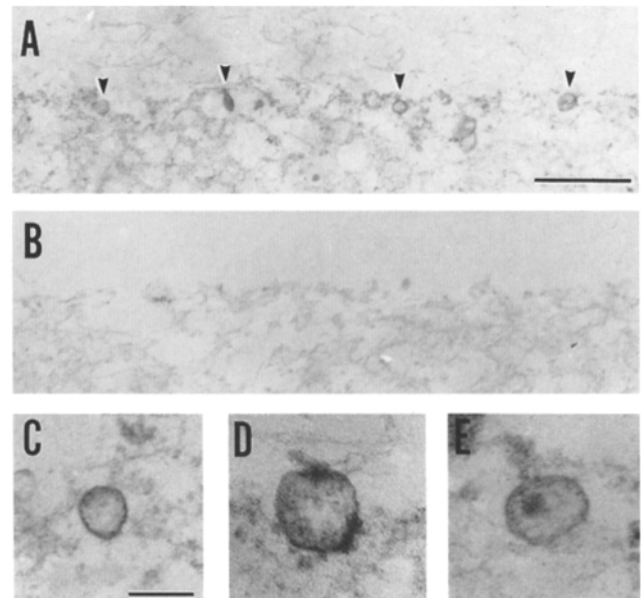

Figure 11. Electron micrographs of affinity-purified KIF3B-associated vesicles. The surface of anti-KIF3B antibody-conjugated (A and C–E) or preimmune rabbit IgG–conjugated beads (B) after being incubated with the crude membrane fraction of cauda equina. At lower magnification, membranous organelles were visible on the anti-KIF3B antibody–conjugated bead (A, arrowheads), but not on the preimmune rabbit IgG–conjugated one (B). Higher magnification (C–E) showed KIF3B-associated vesicles as relatively uniform particles with a diameter of 90–160 nm. Bars: (A and B) 500 nm; (C–E) 100 nm.

ern blot analysis on developing neurons showed a slight difference between the amount of expressed KIF3A and KIF3B mRNA at day 28, while the amount of KIF3A and KIF3B protein showed good agreement in the developmental Western blot. This slight difference suggests that the expression of KIF3A and KIF3B might be regulated at the translation level. In fact, we observed unique characteristics of KIF3B that may explain the mechanism of this regulation: During the purification of recombinant KIF3B and the KIF3A/B complex, KIF3B was found to aggregate under a physiological salt condition, but no such aggregation occurred for KIF3A/B. Since monomeric KIF3A is instead soluble under this condition, when taken together, these findings indicate that monomeric KIF3B may not be able to exist in soluble form in vivo. If true, then heterodimerization with KIF3A may be essential for the stability of KIF3B in vivo. Thus, these findings suggest that these characteristics of KIF3B contribute to the regulation of their expression.

The KIF3 Complex Is a Microtubule-based Plus End–directed Axonal Motor

Previous studies have identified kinesin and cytoplasmic dynein as plus end– (Vale et al., 1985a) and minus end– (Paschal and Vallee, 1987) directed motors in neurons. Although both proteins are attached to axonal membranous organelles, kinesin is preferentially accumulated on the proximal side of a ligated nerve, while cytoplasmic dynein accumulates on both sides of the ligation (Hirokawa et al., 1990, 1991). Our results from the Western blot analysis and immunofluorescence microscopy showed that the KIF3 complex is strongly expressed in neurons. We also found that the KIF3 complex preferentially accumulates on the proximal side of ligated axons, where anterogradely moving organelles accumulate; the motility assay of the recombinant KIF3A/B complex supports this finding.

We hypothesize that the KIF3 complex is a unique motor protein composed of the KIF3A/B heterodimer, and

that it provides another means for anterograde fast axonal transport. Concerning what cargo(es) KIF3 transports, the subcellular fractionation experiments and EM study of immunoprecipitated beads showed that it is ubiquitously associated with membranous organelles, but does not accumulate in synaptic vesicle fractions containing P38. Obviously then, this complex is probably not a motor that specifically transports the synaptic vesicles themselves. However, a possibility nevertheless remains that it associates with the transporting precursor of the synaptic membrane by detaching from the synaptic vesicle at nerve terminals. Because the KIF3 complex exists in various mouse tissues, and may possibly have close homologues with proteins from the sea urchin and Drosophila, a reasonable postulation is that it conveys membranous organelles general to various cell types in vivo. This behavior is supported by the subcellular fractionation data. Future research using appropriate markers is expected to elucidate which cargoes are carried by KIF3.

KAP3 May Regulate the Functions of KIF3 in Various Cell Types

The number of bands and molecular weight of KAP3 were different in the brain and testis. It is thought that kinesin and KIFs that provide transport of membranous organelle have some mechanism for recognizing and binding to cargoes. It has been generally speculated that kinesin light chains play such a role, but no concrete evidence has

proven this. Our evidence that the composition of KAP3 is different in the brain vs testis may support this idea, and this also suggests that its composition in various tissues may be dependent on some functional diversity related to transporting different cargoes.

However, whether this phenomenon is due to a selective association by a distinct polypeptide of KAP3, which is formed by alternative splicing or by other genes' expression; a posttranslational modification, e.g., phosphorylation, in the same polypeptide of KAP3; or simply proteolysis of a single polypeptide of KAP3, remains uncertain. In the case of kinesin, a ~64-kD kinesin light chain was found to be associated with kinesin heavy chains (Vale et al., 1985b; Bloom et al., 1988). Later, several distinct kinesin light chains cDNAs were shown to be formed from alternative splicing of a single gene (Cyr et al., 1991; Gauger and Goldstein, 1993; Wedaman et al., 1993). Thus, multiple light chain proteins can provide a means for generating multiple functionally specialized forms of the kinesin holoenzyme. Therefore, various kinds of KAP3 may be formed by the same mechanism. This finding provides us with new information that can be applied to investigate the association between motor proteins and their cargoes.

The KIF3B Head Itself Has Microtubule Binding and Sliding Activity

We constructed two chimeric KIF3A/B and truncated KIF3A (short 3A) viruses to coinfect with a full-length KIF3B virus using Sf9 cells. Among these altered proteins, a complex with chimera 1 and KIF3B showed microtubule motility in vitro. These results suggest that KIF3B itself has motor activity and does not simply modify KIF3A's motor activity. It is not always necessary to have heterogenous heads for this dimeric motor to generate force. Although this may not happen in vivo, there may be no difference between the functions of KIF3A and KIF3B heads.

Another interesting observation is that a slight difference between two chimeric proteins caused opposite results in motility, though both of them formed a complex with native KIF3B. Chimera 1 has a KIF3B head (amino acid 1–308)/KIF3A rod tail (amino acid 314–701), but chimera 2 has a KIF3B head (amino acid 1–359)/KIF3A rod tail (amino acid 365–701). The difference is only the neck region sequence (amino acid, 3A; 314–368, 3B; 309–363), which connects the head and rod domains; chimera 1 showed microtubule motility whereas chimera 2 did not show it. This implies that a proper neck region is important for dimerization and microtubule motility. Recently, some observations have suggested that the corresponding "neck" region of the kinesin heavy chain is important for protein dimerization (Huang et al., 1994), and such a neck region of myosin is important for force generation. The KIF3A/B complex also seems to be unable to show motility without the right "neck" region. Our results strongly support these investigations.

This study showed that previously reported KIF3A (Kondo et al., 1994) is one component of the KIF3 complex, and this complex actually associates with membranous organelles in nerve axons. We also revealed some molecular mechanism of dimerization and motor activity

of KIF3. The molecular structure of the native KIF3 complex, the primary structure and biochemical characteristics of KAP3, and the precise functions of the KIF3 complex in vivo are intriguing problems that need to be examined in the near future.

References

Aizawa, H., Y. Sekine, R. Takemura, Z. Zhang, M. Nangaku, and N. Hirokawa. 1992. Kinesin family in murine central nervous system. *J. Cell Biol.* 119: 1287–1296.

Banker, G. A., and W. M. Cowan. 1977. Rat hippocampal neurons in dispersed cell culture. *Brain Res.* 126:397–425.

Bloom, G. S., M. C. Wagner, K. K. Pfister, and S. T. Brady. 1988. Native structure and physical properties of brain kinesin and identification of the ATP-binding subunit polypeptide. *Biochemistry.* 27:3409–3416.

Brady, S. T. 1985. A novel brain ATPase with properties expected for the fast axonal transport motor. *Nature (Lond.).* 317:73–75.

Chou, P. Y., and S. D. Fasman. 1974. Prediction of protein conformation. *Biochemistry.* 13:222–245.

Cole, D. G., S. W. Chinn, K. P. Wedaman, K. Hall, T. Vuong, and J. M. Scholey. 1993. Novel heterotrimeric kinesin-related protein purified from sea urchin eggs. *Nature (Lond.).* 366:268–270.

Cyr, J. L., K. K. Pfister, G. S. Bloom, C. A. Slaughter, and S. T. Brady. 1991. Molecular genetics of kinesin light chain: generation of isoforms by alternative splicing. *Proc. Natl. Acad. Sci. USA.* 88:10114–10118.

Endow, S. A. 1991. The emerging kinesin family of microtubule motor proteins. *Trends Biochem. Sci.* 16:221–225.

Garnier, J., D. J. Osguthorpe, and B. Robson. 1978. Analysis of the accuracy and implications of simple methods for predicting the secondary structure of globular proteins. *J. Mol. Biol.* 120:97–120.

Gauger, A. K., and L. S. B. Goldstein. 1993. The *Drosophila* kinesin light chain. *J. Biol. Chem.* 268:13657–13666.

Goldstein, L. S. B. 1991. The kinesin superfamily: tails of functional redundancy. *Trends Cell Biol.* 1:93–98.

Goldstein, L. S. B. 1993. With apologies to scheherazade: tails of 1001 kinesin motors. *Annu. Rev. Genet.* 27:319–351.

Higgins, D. G., A. J. Bleasby, and R. Fuchs. 1992. CLUSTAL V: improved software for multiple sequence alignment. *Comp. Appl. Biosci.* 8:189–191.

Hirokawa, N. 1982. Cross-linker system between neurofilaments, microtubules, and membranous organelles in frog axons revealed by the quick-freeze, freeze-fracture, deep-etching method. *J. Cell Biol.* 94:129–142.

Hirokawa, N. 1993. Axonal transport and the cytoskeleton. *Curr. Opin. Neurobiol.* 3:724–731.

Hirokawa, N., and H. Yorifuji. 1986. Cytoskeletal architecture in the reactivated crayfish axons with special reference to the crossbridges between microtubules and membrane organelles and among microtubules. *Cell Motil. Cytoskeleton.* 6:458–468.

Hirokawa, N., K. K. Pfister, H. Yorifuji, M. C. Wagner, S. T. Brady, and G. S. Bloom. 1989. Submolecular domains of bovine brain kinesin identified by electron microscopy and monoclonal antibody decoration. *Cell.* 56:867–878.

Hirokawa, N., R. Sato-Yoshitake, T. Yoshida, and T. Kawashima. 1990. Brain dynein (MAP 1C) localizes on both anterogradely and retrogradely transported membranous organelles. *J. Cell Biol.* 111:1027–1037.

Hirokawa, N., R. Sato-Yoshitake, N. Kobayashi, K. K. Pfister, and G. S. Bloom. (1991). Membranous organelles in vivo. *J. Cell Biol.* 114:295–302.

Huang, T. G., J. Suhan, and D. D. Hackney. 1994. *Drosophila* kinesin motor domain extending to amino acid protein 392 is dimeric when expressed in *Escherichia coli. J. Biol. Chem.* 269:16502–16507.

Huttner, W. B., W. Schieber, P. Greengard, and P. De Camilli. 1983. Synapsin I, a nerve terminal–specific phosphoprotein. III. Its association with synaptic vesicles studied in a highly purified synaptic vesicle preparation. *J. Cell Biol.* 96:1374–1388.

Johnston, P. A., R. Jahn, and T. C. Sudhof. 1989. Transmembrane topography and evolutionary conservation of synaptophysin. *J. Biol. Chem.* 264:1268–1273.

Kondo, S., R. Sato-Yoshitake, Y. Noda, H. Aizawa, T. Nakata, Y. Matsuura, and N. Hirokawa. 1994. KIF3A is a new microtubule-based anterograde motor in the nerve axon. *J. Cell Biol.* 125:1095–1107.

Nakata, T., R. Takemura, and N. Hirokawa. 1993. A novel member of the dynamin family of GTP-binding protein is expressed specifically in the testis. *J. Cell Sci.* 105:1–5.

Nangaku, M., R. Sato-Yashitake, Y. Okada, Y. Noda, R. Takemura, H. Yamazaki, and N. Hirokawa. 1994. KIF1B, a novel microtubule plus end-directed monomeric motor protein for transport of mitochondria. *Cell.* 79:1209–1220.

Niclas, J., F. Navone, N. Hom-Booher, and R. D. Vale. 1994. Cloning and localization of a conventional kinesin motor expressed exclusively in neurons. *Neuron.* 12:1059–1072.

Noda, Y., R. Sato-Yoshitake, S. Kondo, M. Nangaku, and N. Hirokawa. 1995. KIF2 is a new microtubule-based anterograde motor that transports membranous organelles distinct from those carried by kinesin heavy chain or KIF3A/B. *J. Cell Biol.* 129:157–167.

Okada, Y., R. Sato-Yoshitake, and N. Hirokawa. 1995*a*. The activation of protein kinase A pathway selectively inhibits anterograde axonal transport of vessicle but not mitochondria transport of retrograde transport in vivo. *J. Neurosci.* 15:3053–3064.

Okada, Y., H. Yamazaki, Y. Sekine-Aizawa, and N. Hirokawa. 1995*b*. The neuron specific kinesin superfamily protein KIF1A is a unique monomeric motor for the anterograde axonal transport of synaptic vesicle precursors. *Cell.* 81:769–780.

O'Reilly, D. R., L. K. Miller, and V. A. Luckow. 1992. Baculovirus Expression Vectors, A Laboratory Manual. W. H. Freeman and Company, New York. 109–138pp.

Paschal, B. M., and R. B. Vallee. 1987. Retrograde transport by the microtubule associated protein MAP 1C. *Nature (Lond.).* 330:181–183.

Pesavento, P. A., R. J. Stewart, and L. S. B. Goldstein. 1994. Characterization of the KLP68D kinesin-like protein in *Drosophila*: possible roles in axonal transport. *J. Cell Biol.* 127:1041–1048.

Robson, B., and E. Suzuki. 1976. Conformational properties of amino acid residues in globular proteins. *J. Mol. Biol.* 107:327–356.

Scholey, J. M., M. E. Porter, P. M. Grissom, and J. R. McIntosh. 1985. Identification of kinesin in sea urchin eggs, and evidence for its localization in the mitotic spindle. *Nature (Lond.).* 318:482–486.

Stewart, R. J., P. A. Pesavento, D. N. Woerpel, and L. S. B. Goldstein. 1991. Identification and partial characterization of six members of the kinesin superfamily in *Drosophila. Proc. Natl. Acad. Sci. USA.* 88:8470–8474.

Ueda, T., P. Greengard, K. Berzins, R. S. Cohen, F. Blomberg, D. J. Grab, and P. Siekevitz. 1979. Subcellular distribution in cerebral cortex of two proteins phosphorylated by a cAMP-dependent protein kinase. *J. Cell Biol.* 83:308–319.

Vale, R. D., T. S. Reese, and M. S. Sheetz. 1985*a*. Identification of a novel force-generating protein, kinesin, involved in microtubule-based motility. *Cell.* 42:39–50.

Vale, R. D., B. J. Schnapp, T. S. Reese, and M. S. Sheetz. 1985*b*. Organelle, bead, and microtubule translocations promoted by soluble factors from squid giant axon. *Cell.* 40:559–569.

Wedaman, K. P., A. E. Knight, J. Kendrick-Jones, and J. M. Scholey. 1993. Sequence of sea urchin kinesin light chain isoforms. *J. Mol. Biol.* 231:155–158.